Electronic Supplementary Material (ESI) for Catalysis Science & Technology.

Supporting Information

"Enhancing the hydrogen transfer catalytic activity of hybrid carbon nanotube-based NHC-iridium catalysts by increasing the oxidation degree of the nanosupport"

Matías Blanco,[a] Patricia Álvarez,[a] Clara Blanco,[a] M. Victoria Jiménez[b], Jesús J. Pérez-Torrente,[b] Luis A. Oro,[b] Javier Blasco,[c] Vera Cuartero,[d] and Rosa Menéndez*[a]*

[a] Instituto Nacional del Carbón INCAR-CSIC, P.O. Box 73, 33080, Oviedo, Spain. [b] Department of Inorganic Chemistry, Instituto de Síntesis Química y Catálisis Homogénea (ISQCH-CSIC). University of Zaragoza, 50009, Zaragoza Spain. [c] Instituto de Ciencia de Materiales de Aragón-ICMA, Departamento de Física de la Materia Condensada, CSIC-Universidad de Zaragoza, 50009 Zaragoza, Spain. [d] ESRF-The European Synchrotron, 71, Avenue des Martyrs, Grenoble, France

Extended Characterization of the hybrid carbon nanotube-based NHC-iridium catalysts and nanosupports.

Figure S.10. EXAFS spectra of **CNT-MT-MI-Ir** and IrO_2

Figure S.11. XRD spectra of oxidized carbon materials, hybrid catalysts, and IrO_2 reference sample**.**

Figure S.12-S.16. NMR data for molecular compounds.

References

Table S.1. XPS (atomic percentages), %N (weight percentage) from XPS, % weight loss at *ca.* 400 ºC (TGA measurements), % N weight percentage from TGA. % Ir maximum from TGA %Ir-experimental (ICP measurements), and %Ir load for the hybrid catalysts.

Sample	XPS (Atom %)						XPS (wt)	TGA (wt loss %)	TGA (wt%)	TGA	ICP	%Ir load TGA/ XPS (wt)
	C/O	N	Cl	C	O	S	%N		% N	% Ir max	% Ir exp.	
CNT-HCl	28	0.0	0.0	96.6	3.4	0.0	0.0					
CNT-HCl-MI	23	0.9	0.5	93.7	4.0	0.8	1.0	5.5	1.0			
CNT-HCl-MI-Ir										6.5	3.1	48/49
CNT-LT	20	0.0	0.0	95.2	4.8	0.0	0.0					
CNT-LT-MI	20	1.4	0.6	92.4	4.6	1.0	1.5	7.5	1.4			
CNT-LT-MI-Ir										8.5	6.1	71/66
CNT-MT	16	0.0	0.0	94.1	5.9	0.0	0.0					
CNT-MT-MI	15	1.7	0.8	91.4	6.1	0.0	1.9	8.4	1.6			
CNT-MT-MI-Ir										9.5	10	106/92
CNT-ST	4	0.0	0.0	80.8	19.2	0.0	0.0					
CNT-ST-MI	3.5	2.3	1.3	73.9	21.0	1.5	2.4	11.8	2.3			
CNT-ST-MI-Ir										12.5	12.3	98/94

XPS measurements:

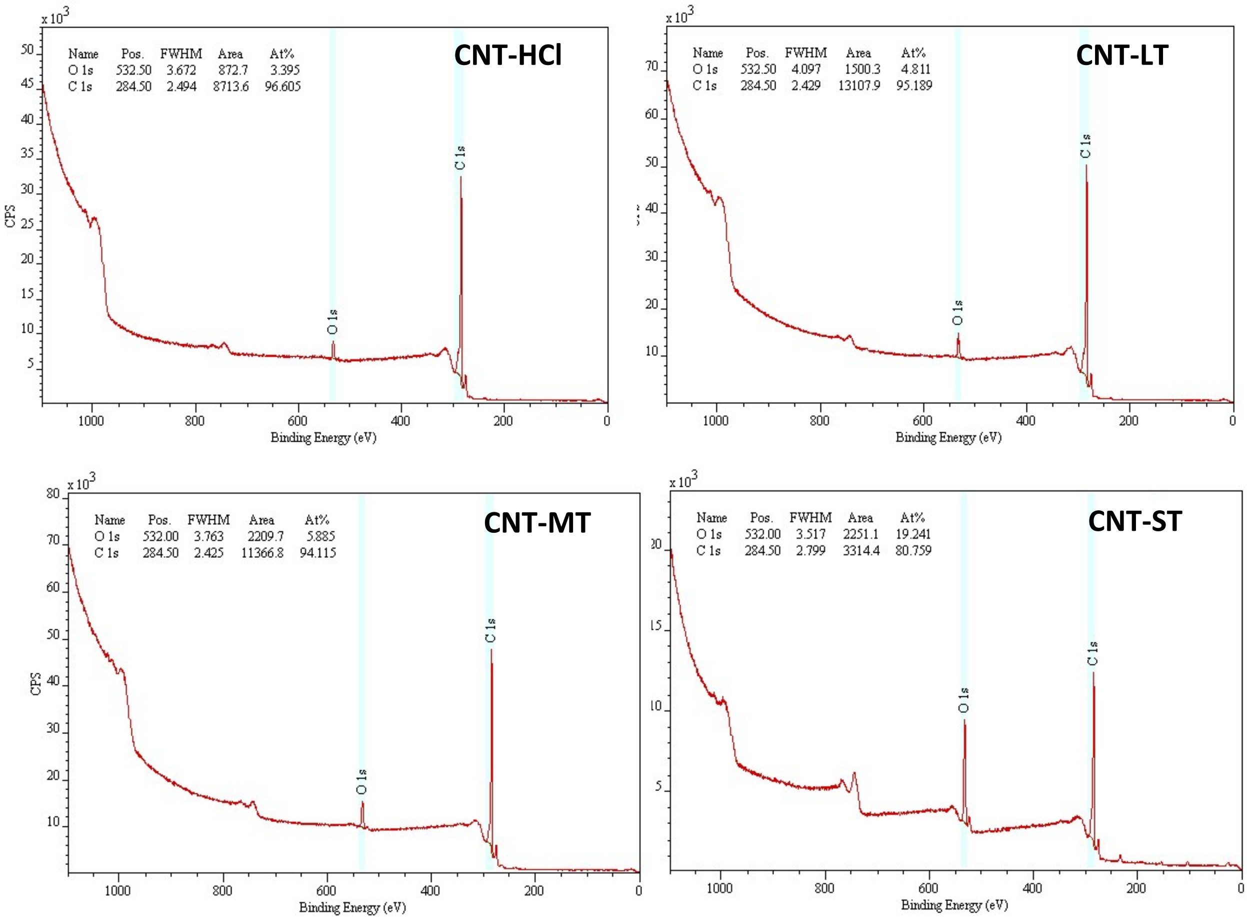

CNT-HCl

Name	Pos.	FWHM	Area	At%
O 1s	532.50	3.672	872.7	3.395
C 1s	284.50	2.494	8713.6	96.605

CNT-LT

Name	Pos.	FWHM	Area	At%
O 1s	532.50	4.097	1500.3	4.811
C 1s	284.50	2.429	13107.9	95.189

CNT-MT

Name	Pos.	FWHM	Area	At%
O 1s	532.00	3.763	2209.7	5.885
C 1s	284.50	2.425	11366.8	94.115

CNT-ST

Name	Pos.	FWHM	Area	At%
O 1s	532.00	3.517	2251.1	19.241
C 1s	284.50	2.799	3314.4	80.759

Figure S.1. General XPS spectra for oxidized carbon materials CNT-X.

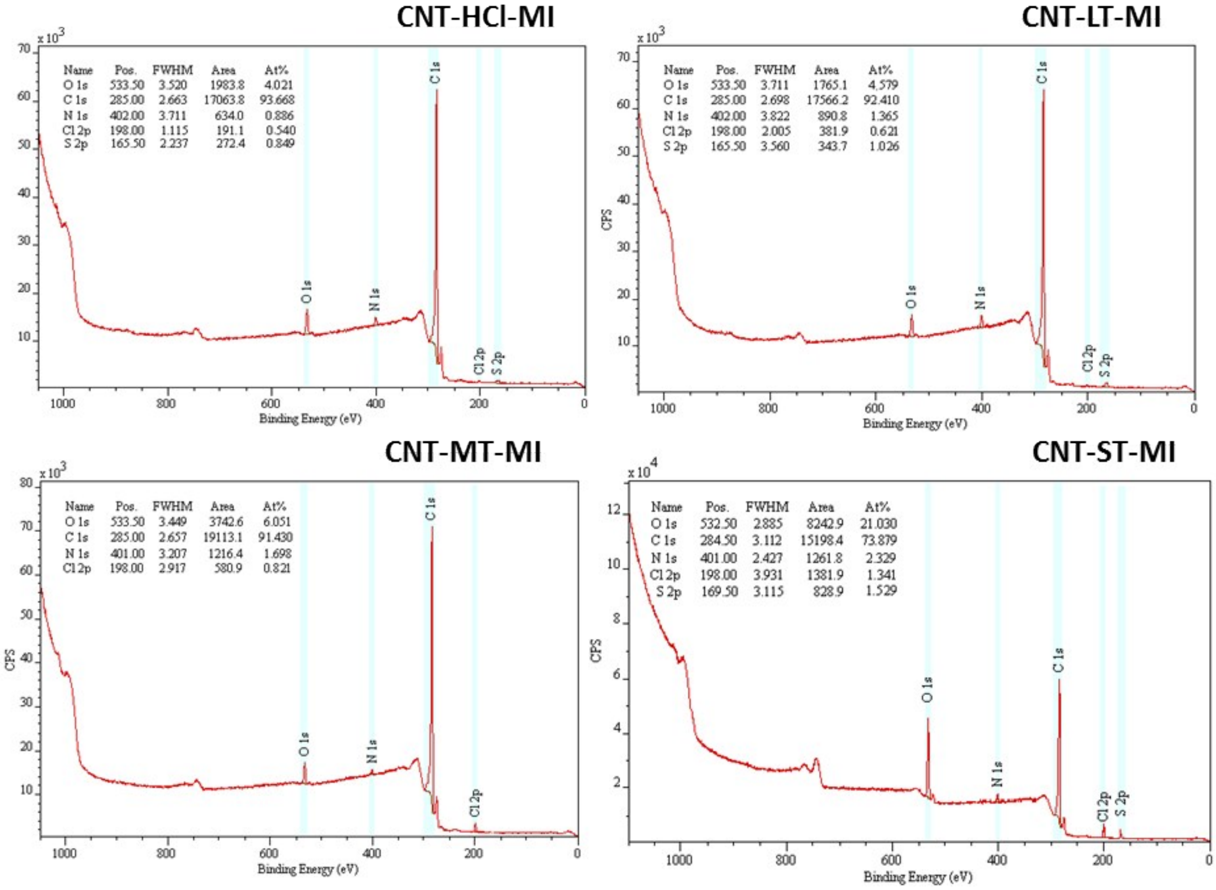

CNT-HCl-MI

Name	Pos.	FWHM	Area	At%
O 1s	533.50	3.520	1983.8	4.021
C 1s	285.00	2.663	17063.8	93.668
N 1s	402.00	3.711	634.0	0.886
Cl 2p	198.00	1.115	191.1	0.540
S 2p	165.50	2.237	272.4	0.849

CNT-LT-MI

Name	Pos.	FWHM	Area	At%
O 1s	533.50	3.711	1765.1	4.579
C 1s	285.00	2.698	17566.2	92.410
N 1s	402.00	3.822	890.8	1.365
Cl 2p	198.00	2.005	381.9	0.621
S 2p	165.50	3.560	343.7	1.026

CNT-MT-MI

Name	Pos.	FWHM	Area	At%
O 1s	533.50	3.449	3742.6	6.051
C 1s	285.00	2.657	19113.1	91.430
N 1s	401.00	3.207	1216.4	1.698
Cl 2p	198.00	2.917	580.9	0.821

CNT-ST-MI

Name	Pos.	FWHM	Area	At%
O 1s	532.50	2.885	8242.9	21.030
C 1s	284.50	3.112	15198.4	73.879
N 1s	401.00	2.427	1261.8	2.329
Cl 2p	198.00	3.931	1381.9	1.341
S 2p	169.50	3.115	828.9	1.529

Figure S.2. General XPS spectra for imidazolium-functionalized carbon materials **CNT-X-MI**.

Table S.2. Deconvolution of the XPS C1s band of the parent carbon nanotube materials

Sample	Csp^2	Csp^3	C-O	C=O	COOH	OCOO
CNT-HCl	78.1	10.9	6.2	2.2	0.8	1.8
CNT-LT	76.1	12.1	3.5	3.5	0.8	2.2
CNT-MT	72.1	14.5	4.3	3.2	2.4	3.3
CNT-ST	66.8	16.6	6.7	2.5	5.0	2.4

The XPS Ir4f region of the spectra of the NHC-iridium supported on the different-oxidation-grade carbon nanotubes are depicted in Figure S.3. Maxima were found at 62.4 eV and 65.6 eV respectively as correspond to iridium (I) species. These results are comparable to those reported before with different Ir(I) NHC complexes supported on carbon nanomaterials by our group.[1]

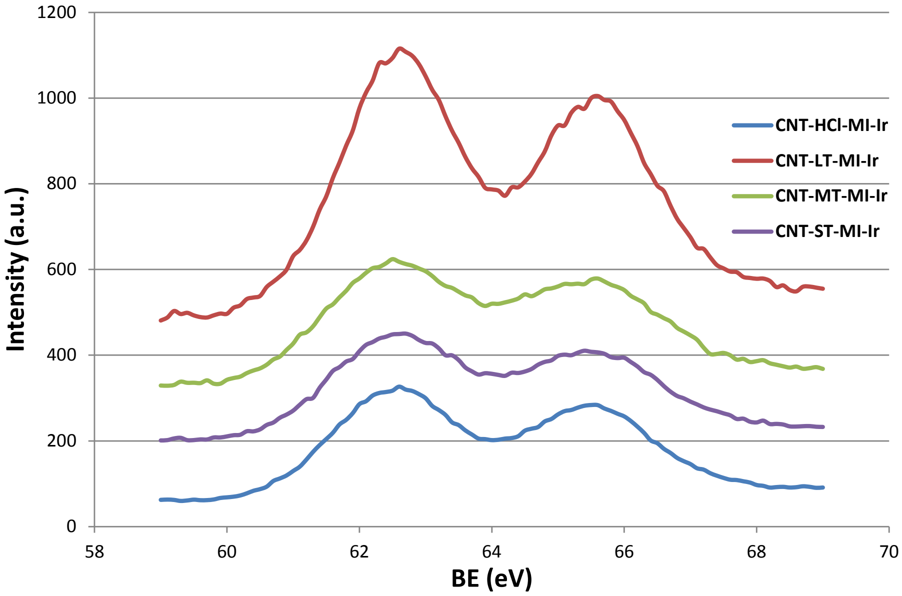

Figure S.3. XPS Ir4f region of the carbon nanotube-based NHC-iridium catalysts.

Thermogravimetric Analyses[2]

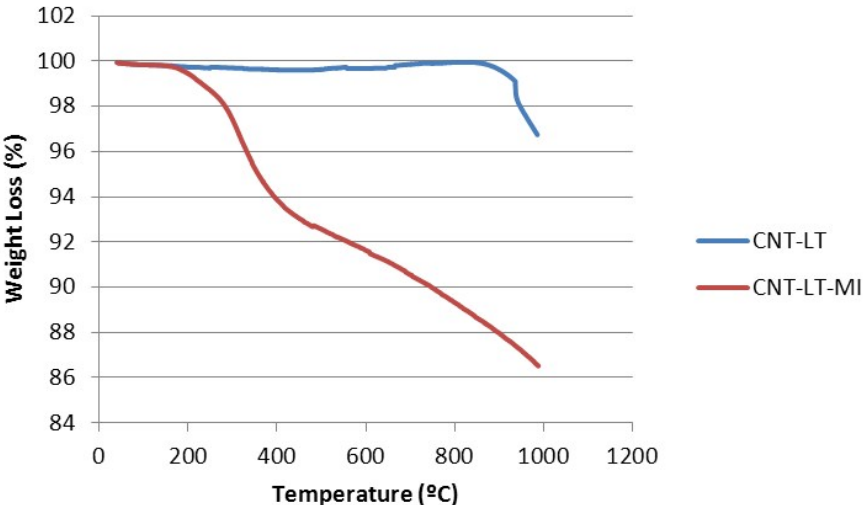

Figure S.4. TGA plots of the oxidized and functionalized nanosupports.

Raman measurements

Raman spectra of parent oxidized and imidazolium functionalized carbon nanotubes are shown in Figure S.1. The characteristic D band (~1340 cm^{-1}), associated to the defects present in the structure, and the graphitic G band (~1580 cm^{-1}) appeared together the typical nanotube pattern. Interestingly, in every case, the D band is increased comparing the functionalized sample with its corresponding parent nanotube material. This effect is commonly reported on the literature as a consequence of the positive functionalization.[3] Table S.1 gathers the ID/IG ratios of parent and functionalized nanotubes

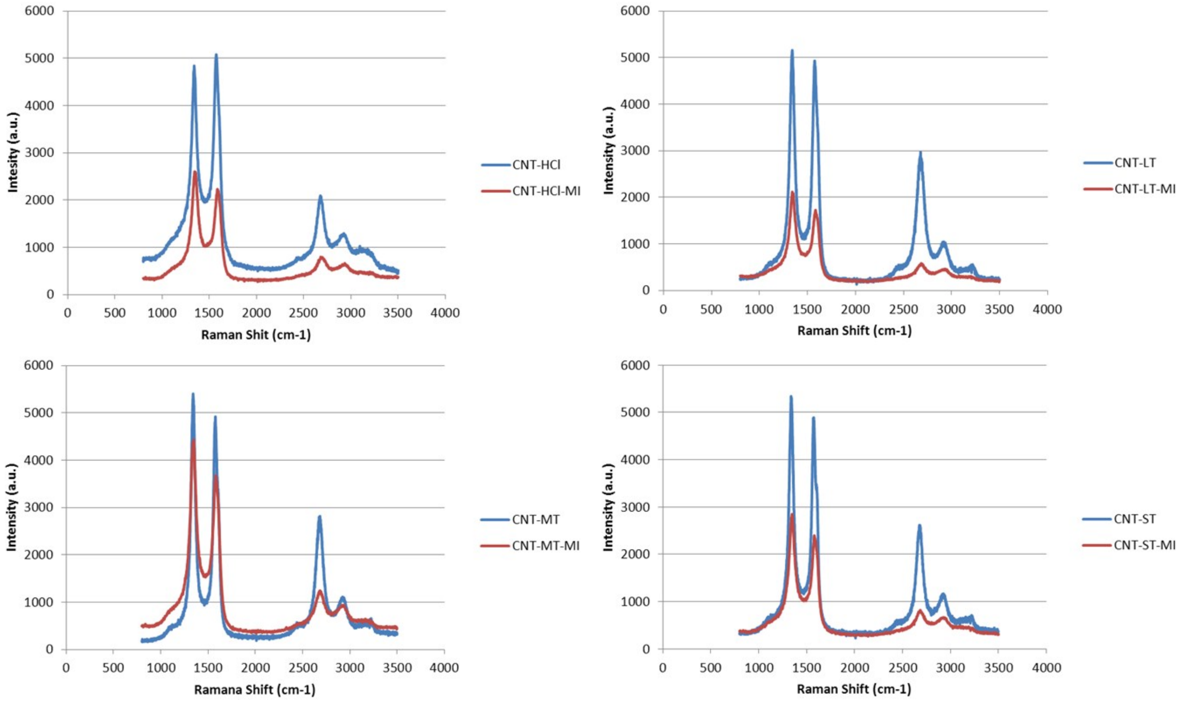

Figure S.5. Raman spectra

Table S.3. Raman ID/IG ratios

Sample	**ID/IG**
CNT-HCl	0.968
CNT-HCl-MI	1.123
CNT-LT	1.047
CNT-LT-MI	1.224
CNT-MT	1.077
CNT-MT-MI	1.213
CNT-ST	1.091
CNT-ST-MI	1.105

Additional TEM images

No additional modifications or residues were found on the materials as a result of the functionalization treatment with the imidazolic compound or the organometallic complex (images on the main text) by comparison with the parent nanotubes.

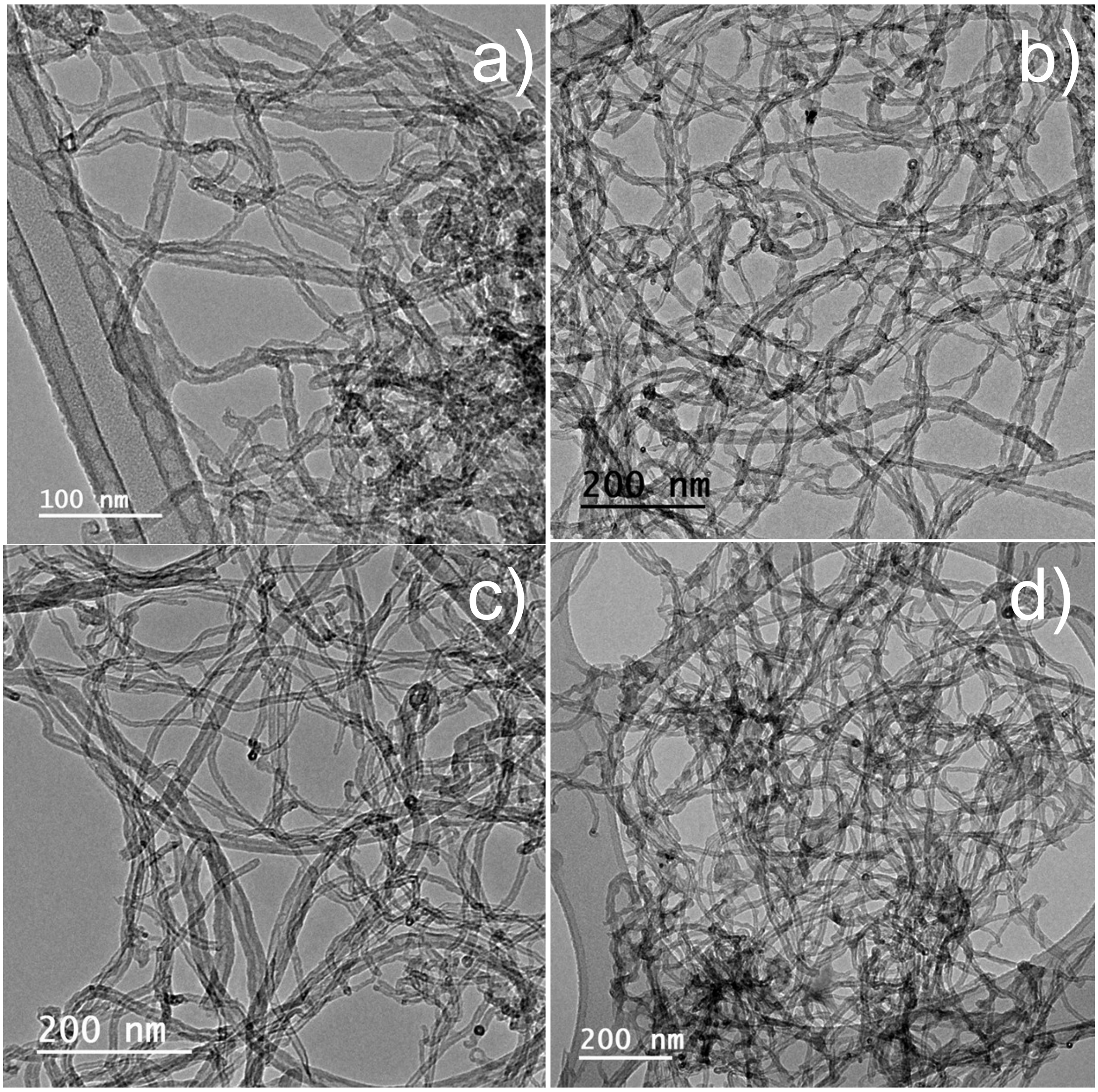

Figure S.6. TEM images of a) **CNT-HCl**, b) **CNT-LT**, c) **CNT-MT** and d) **CNT-ST**

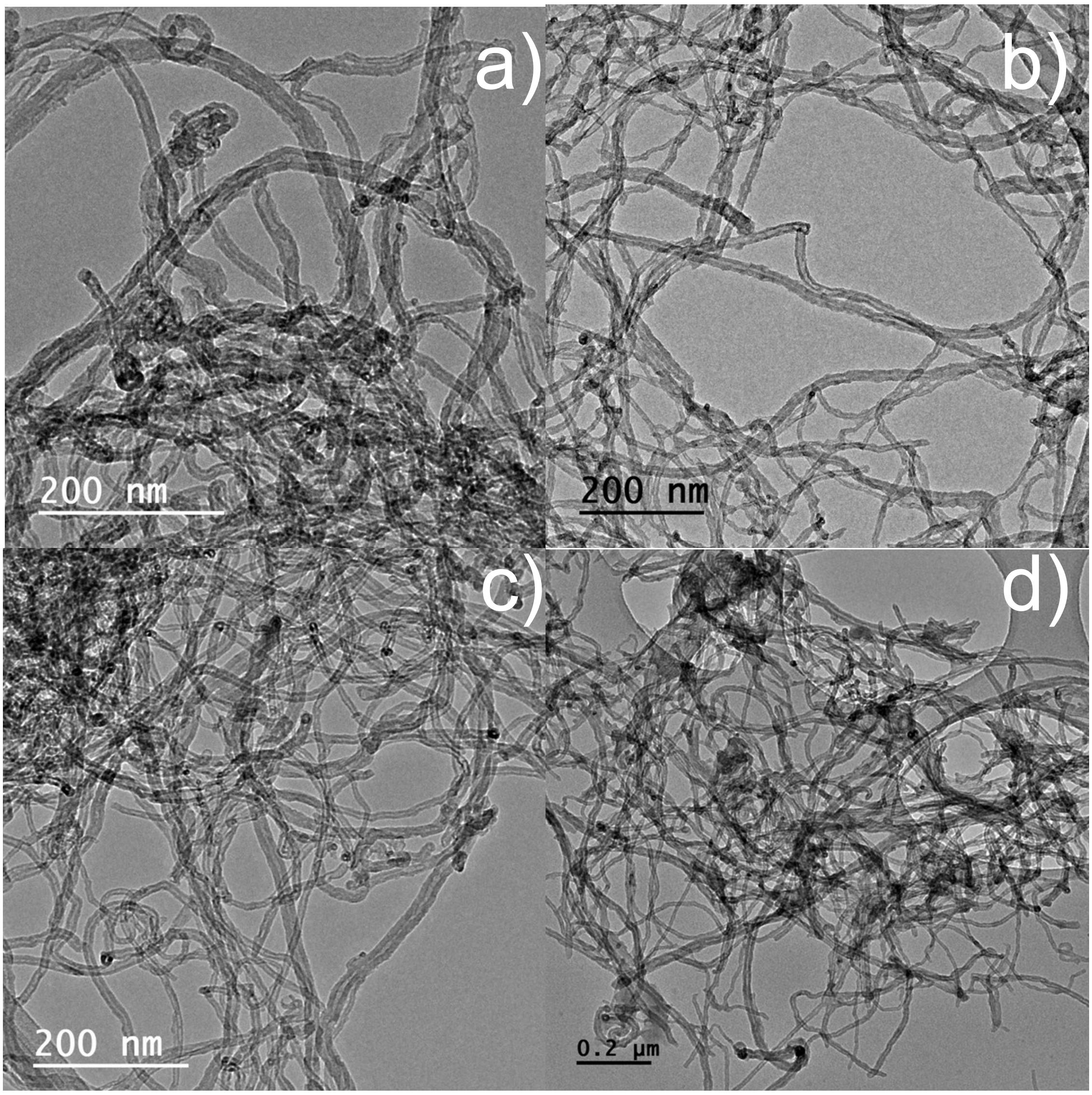

Figure S.7. TEM images of a) **CNT-HCl-MI**, b) **CNT-LT-MI**, c) **CNT-MT-MI** and d) **CNT-ST-MI**

EDX spectra

EDX spectra of the hybrid NHC-iridium complexes supported on the nanotubes are shown in Figure S.5. The iridium atom is clearly detected.

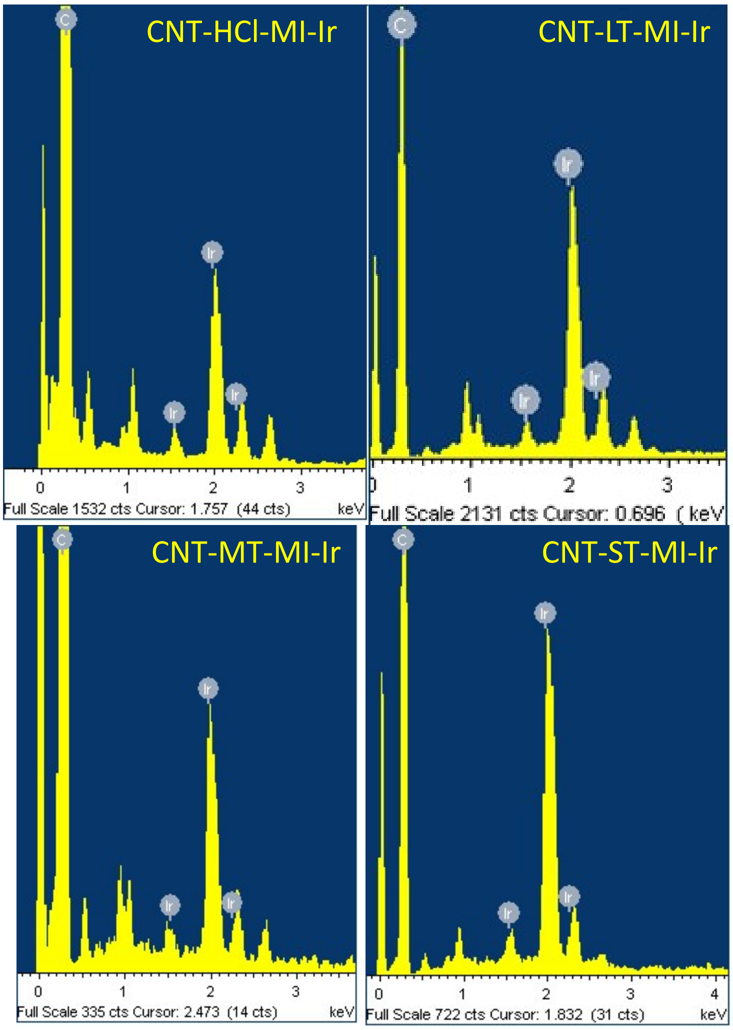

Figure S.8. EDX Spectra of the carbon nanotube-based NHC-iridium catalysts.

Gas Chromatography data

The mother liquids from the reaction of CNT-X-MI with [Ir(μ-OMe)(cod)]$_2$ were analyzed by GC. The presence of methanol was detected as a direct consequence of the deprotonation of the C2 carbon in the imidazolium by the methoxo group. Figure S.7 depicts the chromatographic curves with the control experiment in order to identify that byproduct solvent peak.

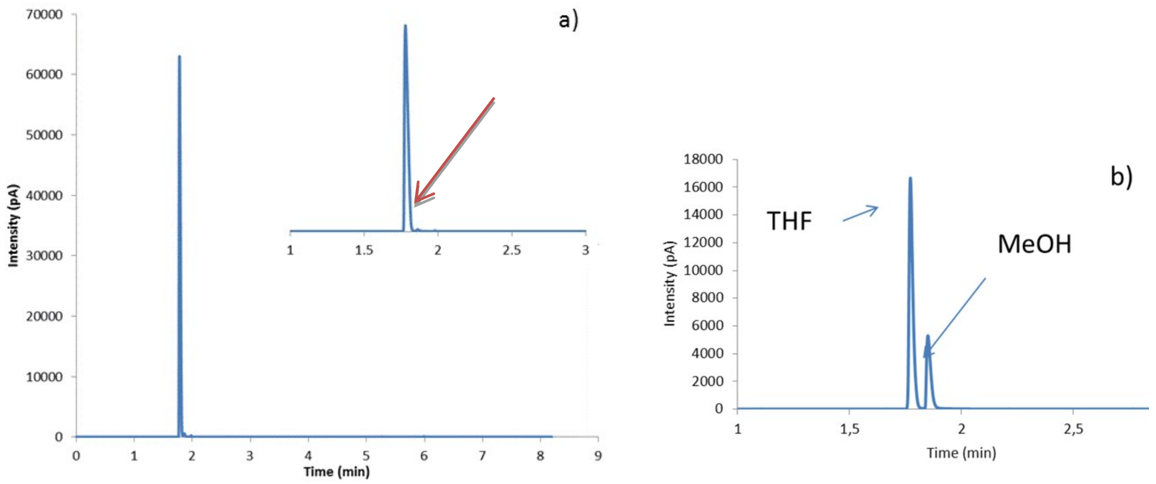

Figure S.9. Chromatographic plots of: a) filtered mother liquid, and b) control experiment.

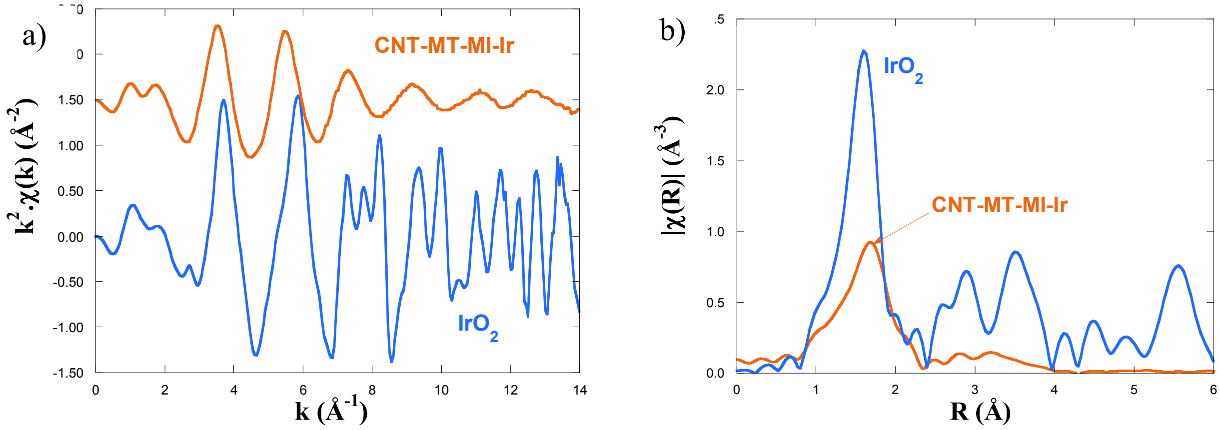

Figure S.10. EXAFS spectra of **CNT-MT-MI-Ir** and IrO_2: a) κ^2-weighted EXAFS spectra of **CNT-MT-MI-Ir** compared with the IrO_2; b) Fourier transform signal from κ^2-weighted EXAFS spectra of **CNT-MT-MI-Ir** and IrO_2; between 3 and 13 $Å^{-1}$.

The EXAFS signal reveals strong differences in the Ir local environment between our catalysts and the IrO_2 reference compound. The difference can also be appreciated in the first layer (intensity and position of the fist peak in the Fourier transform). The iridium is coordinated to six oxygen atoms at the same distance in the IrO_2 compound (within EXAFS accuracy) while the hybrid catalyst **CNT-MT-MI-Ir** have six disordered distances (or different distances). In the next-neighbour atoms, the Ir-Ir paths are clearly noticeable in the peaks around 3 Å lacked in our catalysts. The IrO_2 spectrum is in agreement with previous reports.[4]

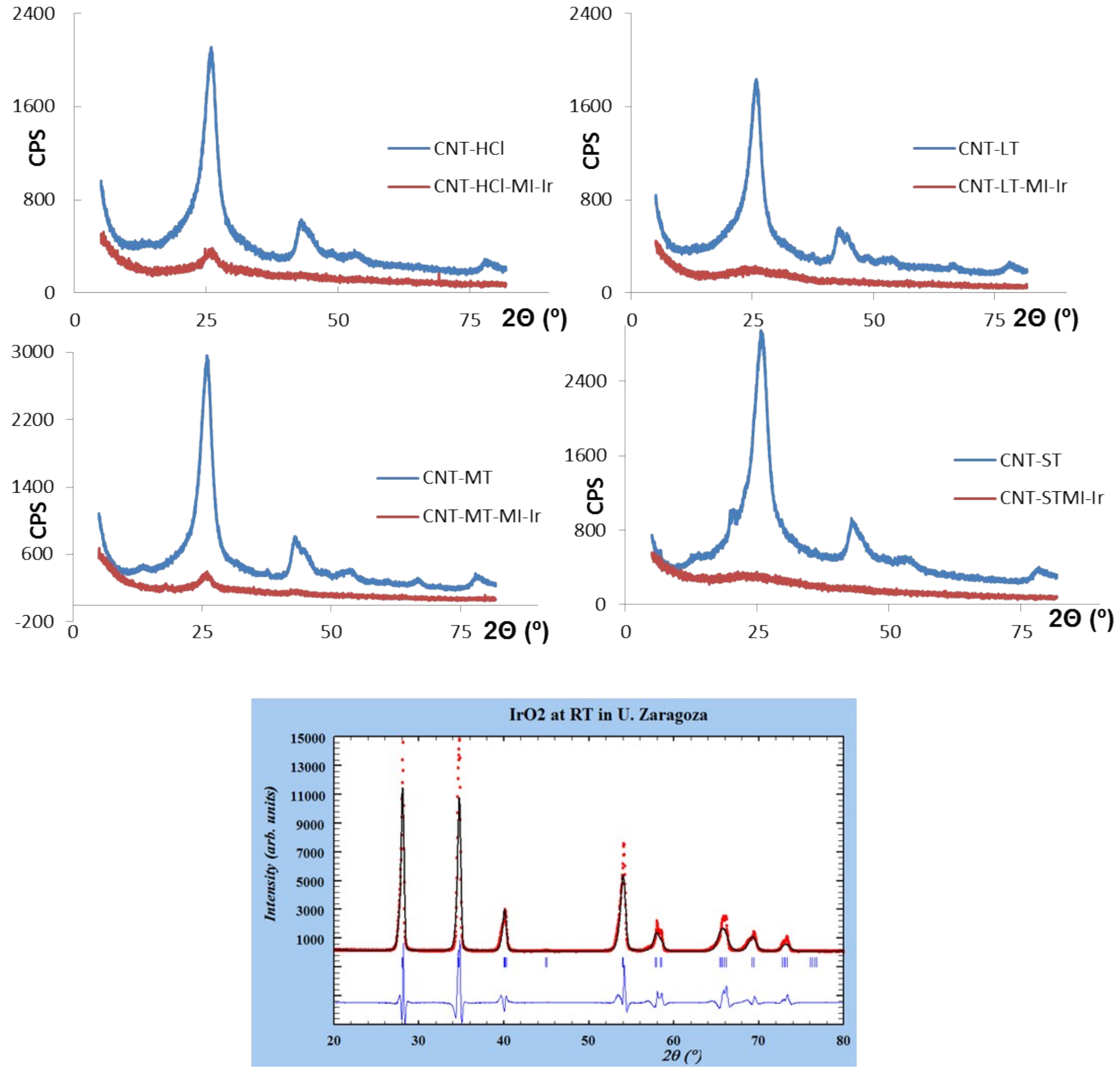

Figure S.11. XRD spectra.

NMR spectra

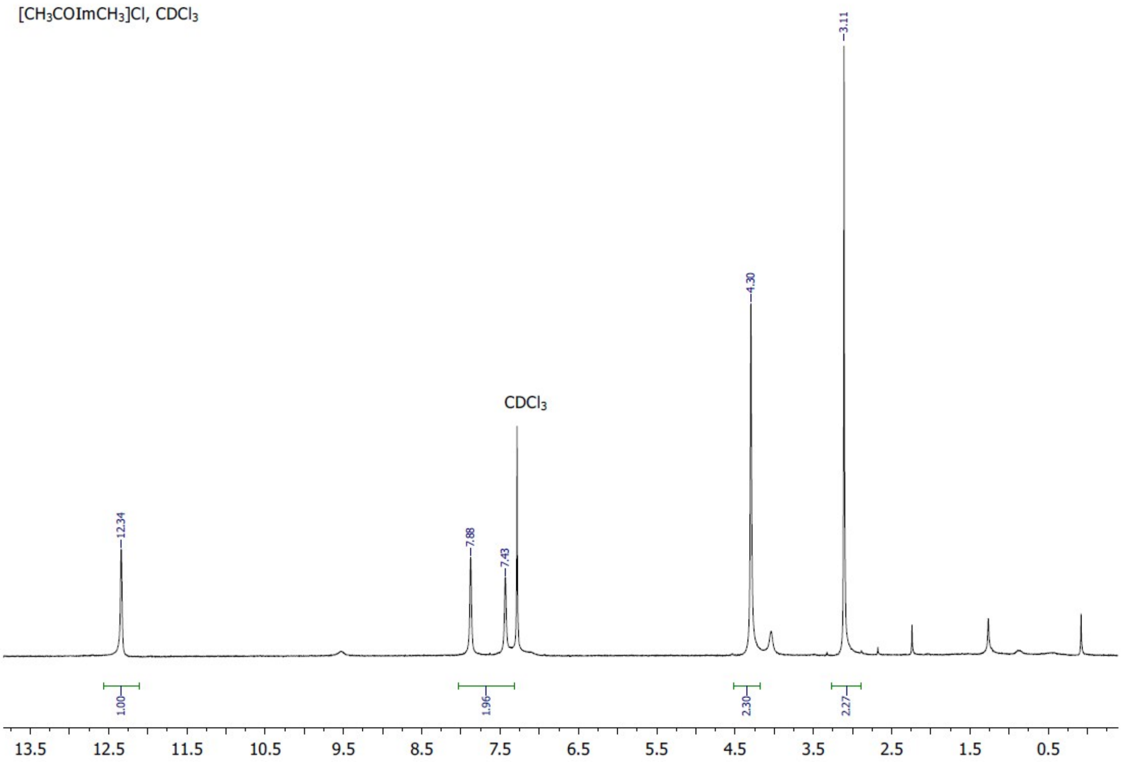

Figure S.12. ^{1}H NMR (C_6D_6, 298K): 1-acetyl-3-methyl-1*H*-imidazol-3-ium chloride

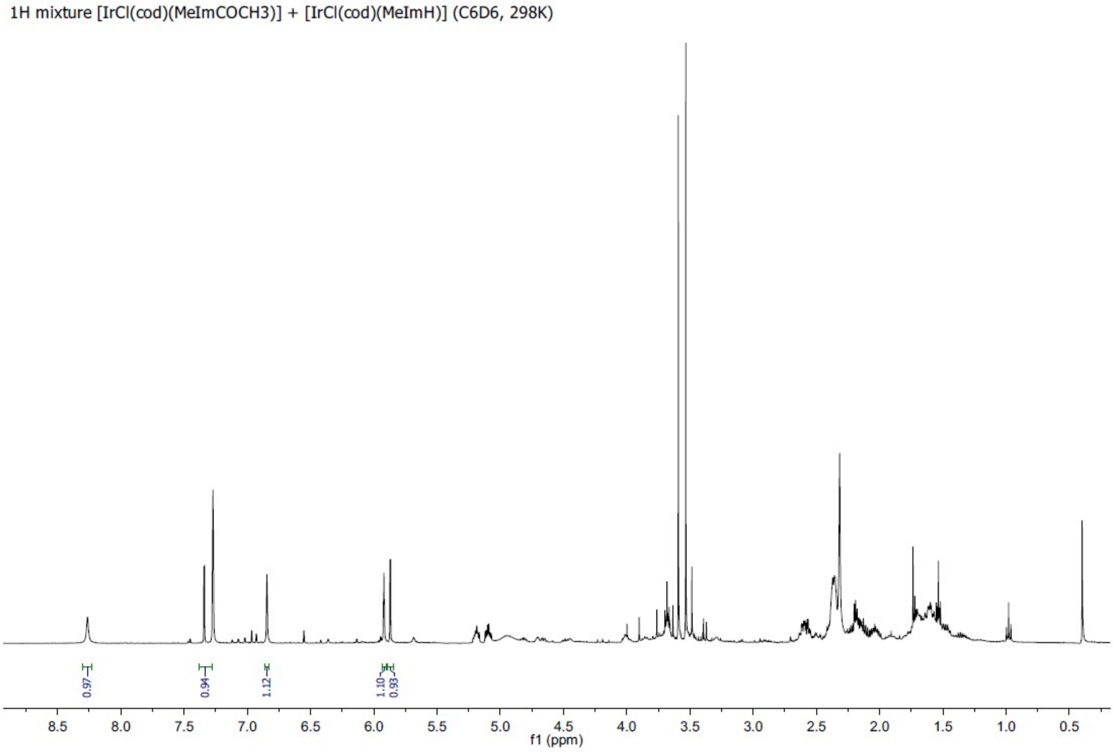

Figure S.13. ^{1}H NMR (C_6D_6, 298K): mixture of [IrCl(cod)(MeImCOCH$_3$)] and [IrCl(cod)(MeImH)]

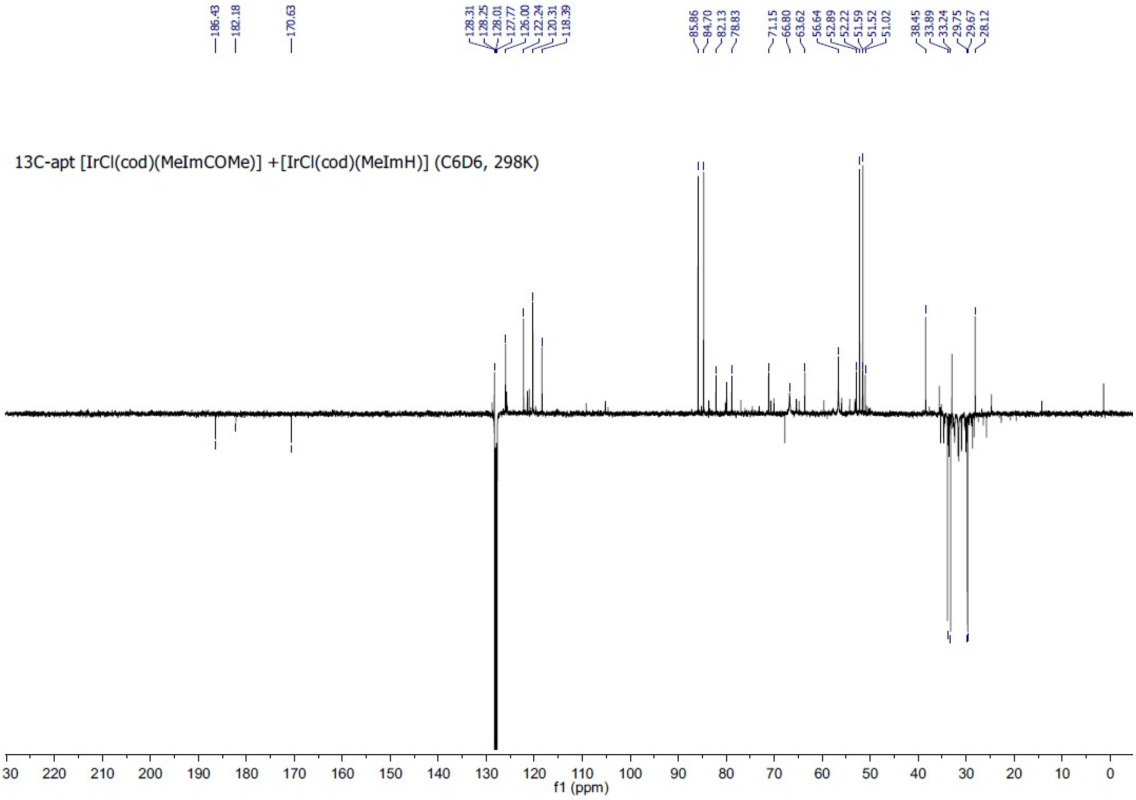

Figure S.14. ^{13}C-apt NMR (C_6D_6, 298K): mixture of [IrCl(cod)(MeImCOCH$_3$)] and [IrCl(cod)(MeImH)]

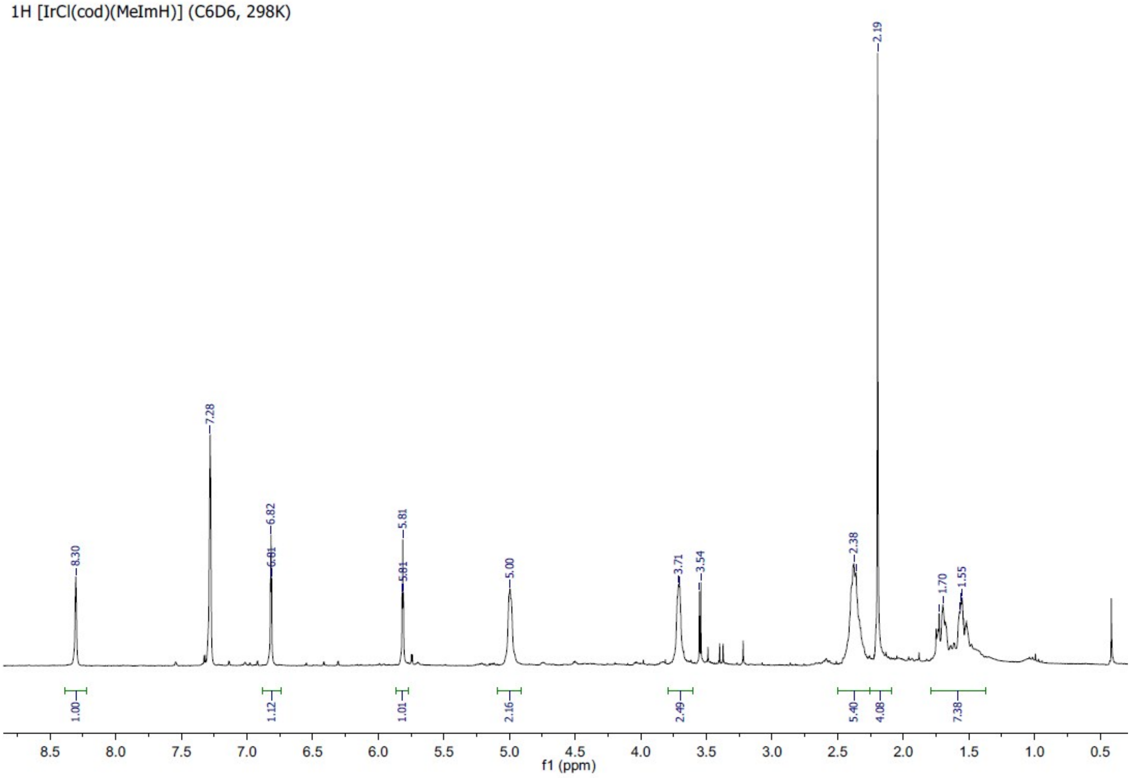

Figure S.15. ^{1}H NMR (C_6D_6, 298K): [IrCl(cod)(MeImH)]

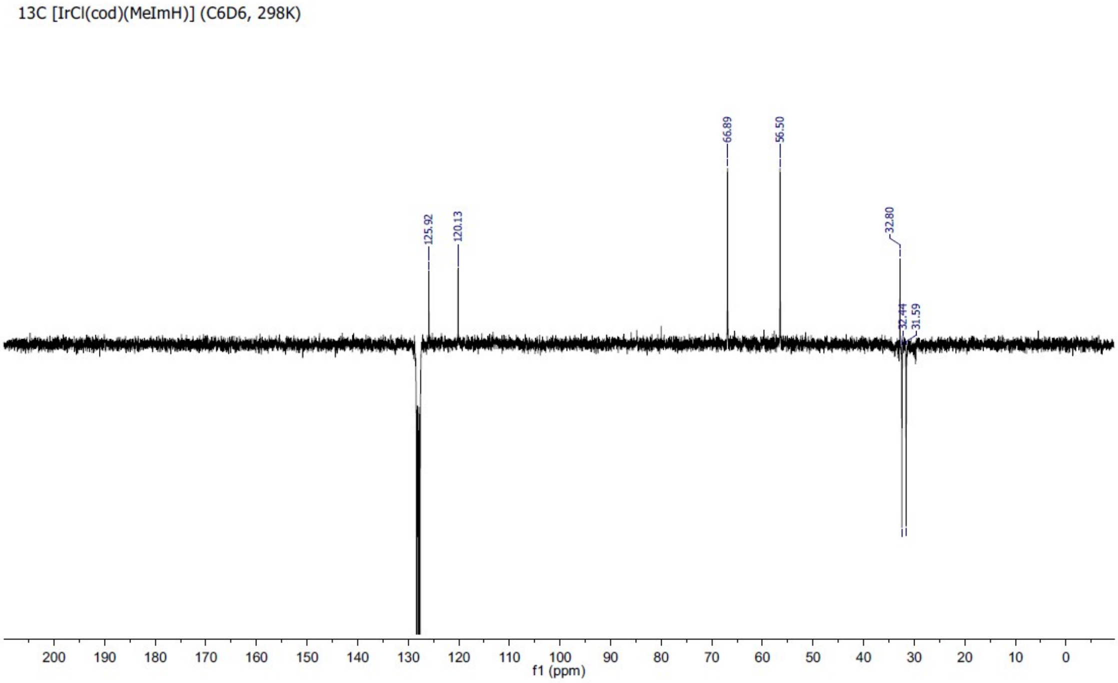

Figure S.16. ^{13}C-apt NMR (C_6D_6, 298K) of [IrCl(cod)(MeImH)]

References

---

[1] M. Blanco, P. Álvarez, C. Blanco. M. V. Jiménez, J. Fernández-Tornos, J. J. Pérez-Torrente, L. A. Oro and R. Menéndez, *Carbon* 2015, **83**, 21−31.

[2] M. J. Park, J. K. Lee, B. S. Lee, Y. W. Lee, I. S. Choi and S. Lee, *Chem. Mater.* 2006, **18**, 1546−1551.

[3] M.S. Dresselhaus, G. Dresselhaus, R. Saito and A. Jorio, *Physics Reports* 2005, **409**, 47–99.

[4] E. Prouzet, *J. Phys.: Condenses Matter*. 1995, **7**, 8027−8033..